

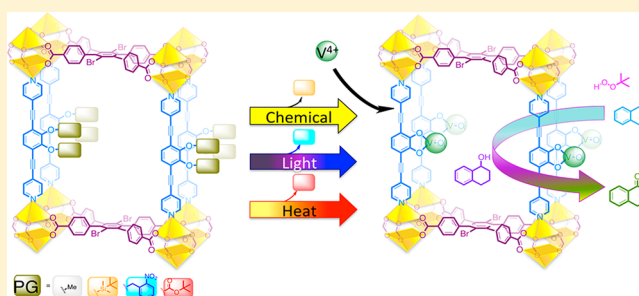
Design, Synthesis, Characterization, and Catalytic Properties of a Large-Pore Metal-Organic Framework Possessing Single-Site Vanadyl(monocatecholate) Moieties

Huong Giang T. Nguyen, Mitchell H. Weston, Amy A. Sarjeant, Daniel M. Gardner, Zhi An, Raanan Carmeli, Michael R. Wasielewski, Omar K. Farha,* Joseph T. Hupp,* and SonBinh T. Nguyen*

Department of Chemistry and the Institute of Catalysis for Energy Processes, Northwestern University, 2145 Sheridan Road, Evanston, Illinois 60208, United States

S Supporting Information

ABSTRACT: Through a combination of protecting groups, postsynthesis deprotection, and postsynthesis metallation, a homogeneously inaccessible, single-site vanadyl(monocatecholate) moiety can be incorporated into the dipyriddy struts of a Zn-based, pillared paddlewheel MOF. The resulting MOF, which has large pores, exhibits catalytic activity in the benzylic oxidation of tetralin in the presence of *tert*-butylhydroperoxide.



INTRODUCTION

As a class of porous and crystalline coordination polymers, metal-organic frameworks (MOFs)^{1–4} are highly promising catalyst scaffolds due to their uniform and well-defined structures and tailorable micropore environments.^{5,6} Because MOFs are microporous materials comprising metal nodes linked together by organic struts, both opportunistic and designed catalysis have been demonstrated at unsaturated metal nodes, at organocatalyst- or metal-complex-tethered organic linkers, as well as through catalysts physically encapsulated by the micropores.^{5–11} While the majority of catalytically active MOFs reported to date contain active metal centers or complexes, these motifs are often pre-existing components of the secondary building units (SBUs) of the MOFs,^{12–14} heterogenized homogeneous catalytic metal complexes,^{15–24} or encapsulated metal complexes^{25–27} or clusters.^{8,28} Examples of MOFs featuring unique metal coordination environments that are inaccessible in solution (or otherwise) remain rare;^{29,30} however, their investigation offers unique opportunities for the development of MOF-based catalysts that can access novel activity or mechanistic pathways.

We and others have previously demonstrated that the single-site activity of homogeneous metalloporphyrin,^{18,21,22,31–33} chiral metallosalen,^{15,17,20} and metalloBINOL^{16,23,24} catalysts, along with their chemo- and enantioselectivities,^{6,11} can be integrated with the shape- and size-selectivity of the MOF environments. Specifically, we have shown that dipyriddy-functionalized analogues of homogeneous porphyrin^{18,22,31} and salen^{15,17} complexes can be synthesized and readily deployed as struts in permanently microporous Zn-based pillared-paddlewheel MOFs that are catalytically active and can be modified

postsynthetically.^{19,22} Herein, we extend this MOF scaffold to display a novel vanadyl(monocatecholate) motif that is catalytically active in a single-site fashion. Unlike metalloporphyrins and metallosalens, this monocatecholate motif is inaccessible in solution because the low-steric coordination environment of the catechol ligand tends to overwhelmingly favor coordinatively saturated bis- and tris-chelate binding modes.³⁴ We hypothesize that the pillared paddlewheel MOF scaffold, constructed from orthogonal carboxylate and dipyriddy struts, would be ideal platforms for spatially isolating catechol-functionalized struts, which can then be postsynthetically metallated to achieve well-defined metal motifs with unsaturated (or labile) coordinative sites capable of novel catalytic behaviors.^{35,36} To achieve MOFs with large pores and apertures, we employ a series of protected catechol-functionalized dipyriddy strut **L1** in combination with the catenation-suppressing³⁷ dibromotetrapopic ligand **L2**. The resulting MOFs can then be deprotected postsynthetically and metallated with vanadium(IV) ions to afford our desired catalytically active MOF materials. To prevent opportunistic catalysis by metal nodes,³⁸ we select redox-inert Zn ions as the structural metal ions.

Because catechol groups readily chelate to Zn ions during crystal growth to form bis- or tris-catecholate homogeneous complexes³⁴ or amorphous coordination networks,³⁹ we started our MOF synthesis with protected catechol struts **L1**. We note that previous attempts, by our groups and others,³⁰ to grow

Received: April 6, 2013

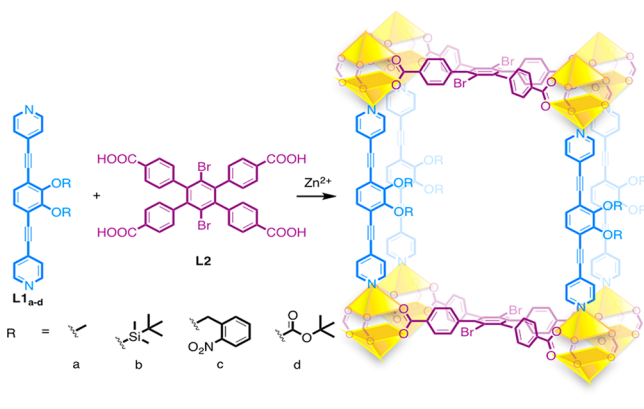
Revised: June 22, 2013

Published: June 25, 2013

MOFs from struts possessing naked catechol moieties have been unsuccessful; even in the best-case scenario where the desired paddlewheel structure can be formed from the unprotected catechol-containing struts, these moieties would readily bind to the residual Zn ions in solution, and the resulting (catecholato)zinc moieties would preclude metallation with other catalytically active metal ions of interest.

Realizing that many deprotection protocols⁴⁰ involve harsh conditions that would degrade most MOFs, we selected protecting groups that can be removed under mild conditions and without compromising the integrity of pillared paddlewheel MOFs. Postsynthesis deprotection^{41–45} studies of MOFs have employed various protecting groups, including fluoride-,^{46,47} photo-,^{30,48–50} and thermo-labile^{51,52} protecting groups, such as trimethylsilyl-, *o*-nitrobenzyl- (*o*NBn-), and *tert*-butoxycarbonyl (BOC), respectively, to mask functional groups that can potentially interfere with de novo MOF synthesis. Thus, we synthesized a series of catechol-containing dipyriddy struts (**L1_{b–d}**) where the catechol moieties are protected with *tert*-butyldimethylsilyl (TBS), *o*NBn, and BOC groups and used them together with **L2** in our MOF synthesis (Scheme 1). As a model, we also synthesized a highly stable MOF from the methyl (Me)-protected derivative **L1_a**.

Scheme 1. A Schematic Illustration of the Solvothermal Synthesis of Zn-Pillared Paddlewheel PG-CatBrO-MOFs



EXPERIMENTAL SECTION

Synthesis of PG-CatBrO MOF (PG = Protecting Group). In a typical synthesis, 1,4-dibromo-2,3,5,6-tetrakis(4-carboxyphenyl)benzene (42 mg, 58.6 μ mol) and $\text{Zn}(\text{NO}_3)_2 \cdot 6\text{H}_2\text{O}$ (34 mg, 114 μ mol) were dissolved via sonication in *N,N*-dimethylformamide (DMF, 8 mL) in an 8 dram vial. **L1_{a–d}** (60 μ mol) was added to the mixture and vortexed until fully dissolved (care was taken to not sonicate these ligands as the sonication energy may be enough to deprotect them). The solution was evenly divided among three 1 dram vials and heated at 75 $^\circ\text{C}$ for at least 24 h to give plate-like crystals that were kept in fresh DMF. See Figure S21 for photographs of **Me-CatBrO MOF** (clear, colorless crystals), **BOC-CatBrO MOF** (amber crystals), ***o*NBn-CatBrO MOF** (yellow crystals), and **TBS-CatBrO MOF** (dark amber crystals).

Synthesis of CatBrO MOF. 1. From *o*NBn-CatBrO MOF. Inside a 4 dram vial, DMF-soaked crystals of ***o*NBn-CatBrO MOF** (~50 mg) were solvent-exchanged to ethyl acetate over a period of 3 days with solvent replacement every 24 h. A portion of the ***o*NBn-CatBrO MOF** (~20 mg) was then transferred into a 1 \times 1 \times 3 cm quartz UV cuvette, capped with a Teflon plug, and irradiated with a Black-ray longwave ultraviolet lamp (model B 100 AP, UVP, San Gabriel, CA, $\lambda = 365$ nm, 115 V, 60 Hz, 2.5A, distance ~10 cm) for 24 h with or without stirring

to give 95% deprotection and minimal deprotection, respectively. Note: Stirring does lead to fragmentation of the crystals.

2. From BOC-CatBrO MOF. Inside a 6 dram vial, DMF-soaked crystals of **BOC-CatBrO MOF** (~50 mg) were solvent-exchanged to 1,2-dichlorobenzene over a period of 3 days with solvent replacement every 24 h. After the last solvent exchange, the whole vial was capped, and the sample was then heated at 140 $^\circ\text{C}$ in a silicone oil bath for 24 h to quantitatively yield free-catechol-bearing **CatBrO MOF**. Complete deprotection was observed through ^1H NMR analysis of a sample of MOF that has been dissolved in a 1:9 v/v mixture of concentrated HCl (aq)/ $\text{DMSO-}d_6$.

Synthesis of V-CatBrO MOF. Inside a 6 dram vial, a sample of **CatBrO MOF** (~50 mg) was solvent-exchanged to tetrahydrofuran (THF) over a period of 2 days with solvent replacement every 12 h. The solvent was then decanted quickly, and to the still-solvated **CatBrO MOF** was added a solution of $\text{VO}(\text{acac})_2$ (50 mg, 189 μ mol) in THF (5 mL). The reaction vial was then capped and heated at 50 $^\circ\text{C}$ in a silicone oil bath for 24 h. The resulting **V-CatBrO MOF** was isolated via decantation, soaked in fresh THF for 1 day at 50 $^\circ\text{C}$, and then soaked in fresh DMF for 3 days at 50 $^\circ\text{C}$ to remove any excess metal ions. ICP analysis indicates that **V-CatBrO MOF** has a V/Zn ratio of 0.35 ± 0.019 , corresponding to ~70% metallation of the catechol groups.

Catalytic Oxidation of Tetralin. In a 5 mL microwave vial (capacity designates the amount of solution that can be safely loaded), catalyst (**V-CatBrO MOF** or **BOC-CatBrO MOF** (4.3 mg (9.6 mg of wet sample based on TGA determination of the amount of solvent uptake), 2.5 μ mol of V for **V-CatBrO MOF**) or $\text{VO}(\text{acac})_2$ (0.66 mg, 2.5 μ mol)), tetralin (34.1 μL , 33.1 mg, 0.25 mmol), and tribromobenzene (20 mg, 0.064 mmol, as an internal standard) were combined in chlorobenzene (3 mL). *tert*-Butyl hydroperoxide (0.043 mL of a 5–6 M solution in nonane; a 6 M solution is assumed for TON calculation) was slowly added dropwise over 10 s. The reaction vial was sealed with a Teflon-lined cap and allowed to shake at 200 rpm and 50 $^\circ\text{C}$ in a Thermolyne Type 17600 aluminum heating block (Thermolyne, Dubuque, IA) mounted on a Thermolyne Type 65800 shaker (Thermolyne, Dubuque, IA). Aliquots from the reaction mixture (~0.1 mL) were regularly collected using a syringe and diluted to 1 mL with dichloromethane in a GC vial before being analyzed with gas chromatography.

Gas chromatography was performed on an Agilent Technologies 6890N Network GC system equipped with an FID detector and HP-5 capillary column (30 m \times 320 μm \times 0.25 μm film thickness). Analysis parameters were as follows: initial temperature = 50 $^\circ\text{C}$, initial time = 3 min, ramp = 10 $^\circ\text{C}/\text{min}$, final temperature = 200 $^\circ\text{C}$, final time = 10 min. Elution times (min) = 12.7 (tetralin); 15.8 (tetralol); 16.2 (α -tetralone); 16.9 (tribromobenzene, internal standard); oxidation product concentration was calculated on the basis of calibration curves using tribromobenzene as the internal standard.

Determination of Potential Catalyst Leaching via Filtration.

At the 4 h point into a typical oxidation run (see above), the reaction mixture was removed from the shaker, and catalyst crystals were allowed to settle at the bottom of the microwave vial. The supernatant was gently removed via a syringe equipped with a fine needle, leaving behind the catalyst, and filtered through a 0.1 μm filtration disk into a new microwave vial. The filtrate was allowed to react further at 50 $^\circ\text{C}$ on the shaker and monitored by gas chromatography by removing aliquots from the reaction mixture (~0.1 mL) using a syringe. Each aliquot is diluted with dichloromethane to 1 mL in a GC vial before being analyzed.

Single-Crystal Structure Determination. A single crystal of $\text{C}_{56}\text{H}_{30}\text{Br}_2\text{N}_2\text{O}_{10}\text{Zn}_2$ [**Me-CatBrO-MOF**, designated as n1694 in the CIF], isolated from a sample of freshly grown MOFs in DMF, was mounted in inert oil and transferred to the cold gas stream of a Bruker Kappa APEX CCD area detector equipped with a Cu K_α microsource and MX optics. Absorption correction was carried out using SADABS-2008/1 (Bruker, 2008) ($R(\text{int})$ was 0.1061 before and 0.0755 after correction). The ratio of minimum to maximum transmission is 0.7660. The $\lambda/2$ correction factor is 0.0015. See Table S1 in the Supporting Information for additional information.

A single crystal of $C_{54}H_{36}N_6O_{20}Zn_2$ [BOC-CatBrO MOF, designated as n2053 in the CIF], isolated from a sample of freshly grown MOFs in DMF, was mounted in inert oil and transferred to the cold gas stream of a Bruker Kappa APEX CCD area detector equipped with a Cu K_{α} microsource and Quazar optics. Absorption correction was carried out using SADABS-2008/1 (Bruker, 2008) (wR2(int) was 0.0639 before and 0.0533 after correction). The ratio of minimum to maximum transmission is 0.8948. The $\lambda/2$ correction factor is 0.0015. See Table S2 in the Supporting Information for additional information.

RESULTS AND DISCUSSION

MOF Synthesis and Characterization. PG-CatBrO MOFs were solvothermally synthesized from $Zn(NO_3)_2 \cdot 6H_2O$, L2, and $L1_{a-d}$ in DMF (Scheme 1) to give plate-like colorless to amber crystals. TGA analyses of these as-synthesized MOFs suggest that they have large solvent-accessible pores (~ 45 – 55 wt % of trapped DMF solvent) and high thermal stability (decomposition at 450 °C) (Figure S22 in the Supporting Information).

Unfortunately, only the structures of Me-CatBrO MOF and BOC-CatBrO MOF were fully determined; that of NBn-CatBrO MOF was only partially resolved, and that of TBS-CatBrO MOF could not be obtained due to weak diffraction. Figure 1 shows the full structures of Me- and BOC-CatBrO

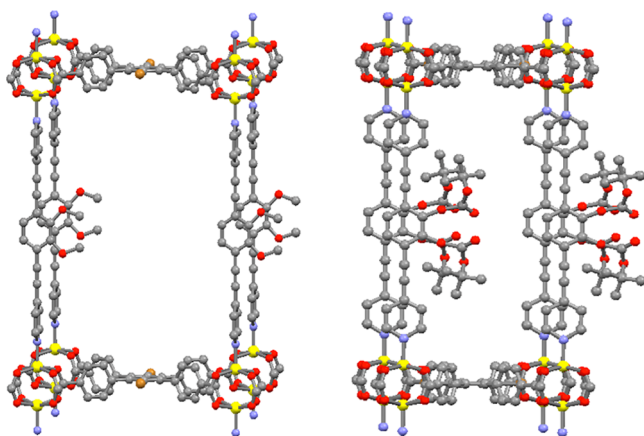


Figure 1. Ball-and-stick depiction of the structures of Me-CatBrO MOF (left) and BOC-CatBrO MOF (right) as determined by single-crystal X-ray diffraction. The BOC groups are disordered and are only shown in representative locations, reflecting their 50% occupancy probability (i.e., they occupy two of the four positions around that central phenyl ring of the dipyriddyil struts). Gray = C, red = O, blue = N, yellow = Zn. All H atoms have been omitted for clarity.

MOFs, which consist of L1 pillars linking xy -oriented 2-D sheets of Zn(II) dimers bridged by ligand L2. The available single-crystal X-ray diffraction data for *o*NBn-CatBrO MOF showed that it crystallizes in the same space group $Pm\bar{3}m$ as Me- and BOC-CatBrO MOFs and share the same unit cell ($a = 11$; $b = 16$; $c = 23$ Å). In addition, the PXRD patterns of all four MOFs agree with the simulated pattern for Me-CatBrO MOF, indicating that they are isostructural (Figure 2).

Consistent with the formula $[Zn_2(L1_a)(L2)]$, obtained from X-ray diffraction, the NMR spectra of a sample of concentrated D_2SO_4 -digested Me-CatBrO MOF showed a 1:1 ratio of $L1_a:L2$ (Figure S31 in the Supporting Information). Unfortunately, D_2SO_4 digestion of the remaining PG-CatBrO MOFs partially degraded the acid-labile protecting groups in $L1_{b-d}$ struts and decomposed the redox-active catechol group, making it difficult to obtain quantitative stoichiometric data through

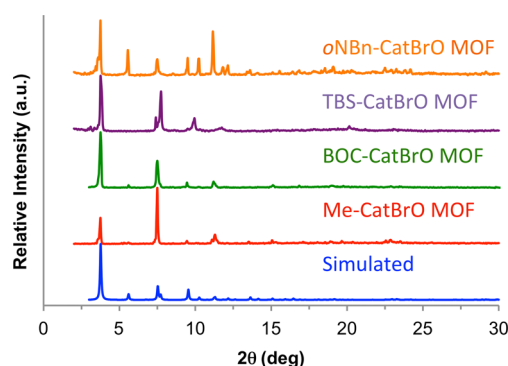


Figure 2. PXRD patterns of simulated (bottom to top) PG-CatBrO MOFs (blue), Me-CatBrO MOF (red), BOC-CatBrO MOF (green), TBS-CatBrO MOF (purple), and *o*NBn-CatBrO MOF (orange).

integration of the dipyriddyil protons against those of L2. For digested *o*NBn-CatBrO MOF, a ~ 1.3 :1 molar ratio of $L1_c:L2$ could be obtained if integration was based on the benzylic protons of the nitrobenzyl groups (Figure S32 in the Supporting Information). For BOC-CatBrO MOF, digestion in a milder solution of concentrated HCl:DMSO- d_6 (1:9 v/v) was a good alternative, showing a (0.6 ± 0.1) :1 ratio for $L1_d:L2$ (Figure S33 in the Supporting Information; see Figure S34 in the Supporting Information for deviation in ratio after deprotection).

Postsynthesis Deprotection of PG-CatBrO MOFs. Surprisingly, the 1H NMR spectrum of concentrated D_2SO_4 -digested TBS-CatBrO MOF (Figure S35 in the Supporting Information) shows that the TBS ether was deprotected in situ during MOF synthesis, an observation that is supported by the absence of Si in its ICP-OES data. ICP analysis of a dry sample of TBS-CatBrO MOF further indicated that the deprotected catechol groups are also chelated to Zn (16.1 wt % Zn expected for Zn-CatBrO MOF, 17.8 wt % Zn observed). As Kitagawa and co-workers,⁴³ and later Rankine et al.,⁴⁴ have seen similar in situ deprotection of acetyl esters during MOF synthesis, it is possible that the slightly acidic solvothermal conditions that we used to synthesize TBS-CatBrO MOF could be responsible for the in situ desilylation. Because our goal was to obtain free catechol moieties that could be metallated with V^{IV} ions postsynthesis and the deprotection of Me-CatBrO MOF would require a vigorous and framework-degrading reaction with BBr_3 , we explored the photolabile *o*NBn- and the thermolabile BOC-protecting groups.

Following a procedure reported by Cohen and co-workers,³⁰ a sample of *o*NBn-CatBrO MOF in EtOAc was irradiated at 365 nm for 24 h. Unfortunately, complete photodeprotection, as determined by NMR spectroscopic analysis of concentrated D_2SO_4 -digested MOF samples, was not achieved when the crystals were not stirred, probably due to a combination of light scattering by the MOF crystals and incomplete light penetration. Stirring the crystals led to 95% deprotection (Figure S36 in the Supporting Information), but also broke the sample down to powdery microcrystallites (Figure S38 in the Supporting Information). Thus, while the photochemical deprotection of the photolabile *o*NBn protecting group does not chemically degrade the MOF, mechanical stress leading to crystal fragmentation was unavoidably incurred. Although smaller crystallites will increase the percentage of external surface area relative to internal pore surface, and may be advantageous in cases where catalysis is mostly limited to

surface, they also diminish the ability to distinguish surface versus internal catalysis. As such, a protecting group that can be removed without leading to crystal fragmentation is preferred when size-, shape-, or enantioselectivities offered by the pores of the MOF are desired.

Fortunately, the thermolabile BOC protecting group does offer a facile path for “traceless” deprotection,⁵¹ as shown by the TGA profile of **L1_d** (Figure S39 in the Supporting Information), which indicates ~35% mass loss starting at 130 °C, corresponding to the thermolysis of the BOC groups. As the TGA plot of **BOC-CatBrO MOF** activated at room temperature under vacuum (to preserve the thermolabile BOC groups) shows an initial mass loss step (~12%, Figure S40 in the Supporting Information), which we attributed to the BOC group (theoretical BOC group mass % = 15%), and the components of **PG-CatBrO MOFs** are thermally stable up to 450 °C (see TGA discussion above), this relatively low deprotection temperature should not pose a problem. Indeed, the BOC groups could be removed by carrying out the deprotection of **BOC-CatBrO MOF** in 1,2-dichlorobenzene at 140 °C. Removal of the BOC group was confirmed by the ¹H NMR spectrum of a concentrated HCl/DMSO-*d*₆-digested MOF sample (Figure 3). In addition, the FTIR spectrum of

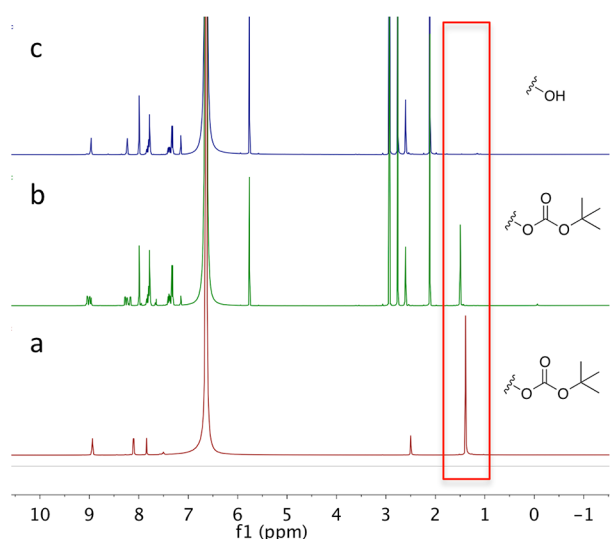


Figure 3. ¹H NMR spectra in concentrated HCl/DMSO-*d*₆ (1:9 v/v) of (a) **L1_d**, (b) **BOC-CatBrO MOF**, and (c) **CatBrO MOF**, highlighting the disappearance of the *tert*-butyl protons at 1.5 ppm (boxed region) in (c). The complex splitting pattern of the aromatic protons in (b) indicates a possible mixture of di- and monoprotected **L1_d** as well as deprotected **L1_d** in the **BOC-CatBrO MOF**. Integration of *tert*-butyl protons in (b) relative to aromatic protons of **L1_d** indicates 1/4 of BOC groups are cleaved. See Figure S33 in the Supporting Information for further analysis.

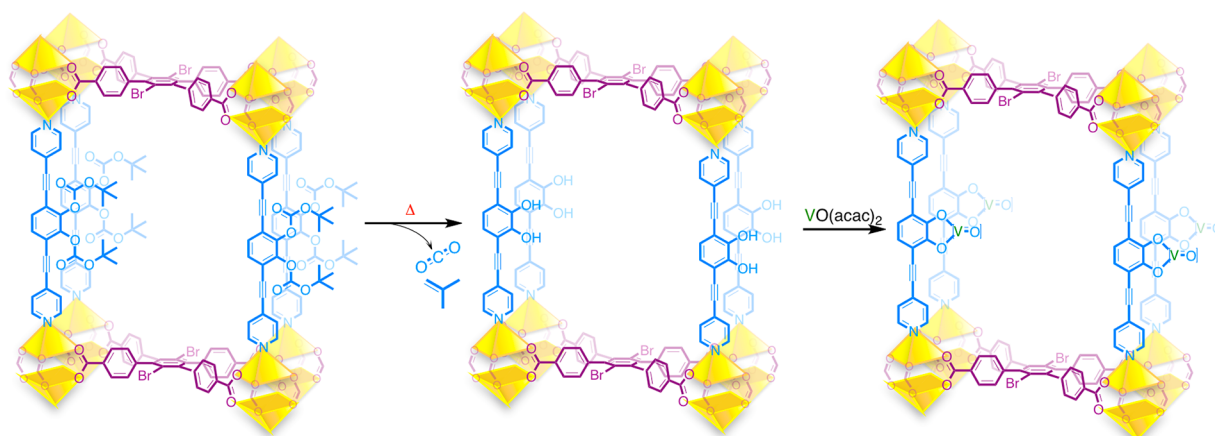
CatBrO MOF indicated the complete disappearance of the C=O stretch of the BOC group around 1775 cm⁻¹ after thermal treatment (Figure S42 in the Supporting Information). The PXRD pattern of the deprotected **CatBrO MOF** (Figure S43 in the Supporting Information), which is quite similar to that of the starting materials, showed that the crystallinity of the framework was maintained. This is further supported by the observation that the TGA profile of **CatBrO MOF** is also very similar to that of **BOC-CatBrO MOF**, showing ~55 wt % loss before 450 °C (Figure S44 in the Supporting Information). Because the trapped DMF solvent molecules are removed from

the solvent-wetted (i.e., unactivated) MOF crystals at a temperature that is similar to that of the BOC deprotection, we cannot completely distinguish these two processes by TGA. However, it is possible that the volume vacated by the BOC groups in **CatBrO MOF** is replaced by solvent molecules, resulting in a mass loss similar to that of **BOC-CatBrO MOF**.

Metallation of Catechol Group. Given that the deprotection of **BOC-CatBrO MOF** afforded unfragmented crystals of **CatBrO MOF**, we proceed to metallate it with VO(acac)₂ in THF to give the metallated derivative **V-CatBrO MOF**, with metal loadings as high as 0.72 V/catechol (average = 0.35 V/Zn, expected 0.5 V/Zn) as determined by ICP-OES analysis (Scheme 2). The TGA profile of the metallated MOF appears nearly unchanged from the parent MOF, indicating retention of large solvent-accessible pores that can facilitate catalysis (Figure S44 in the Supporting Information). Metallation in MeOH, DMF, *t*-BuOH, and dioxane did not work as well, yielding materials with either low metal loadings or reduced crystallinity (Table S4 and Figure S43 in the Supporting Information). As a control, subjecting **BOC-CatBrO MOF** to the same metallation procedure in THF resulted in low metal loading (0.07 V/Zn), further confirming the importance of the catechol moiety for binding the vanadyl ion.

Analysis of **V-CatBrO MOF** using X-ray photoelectron spectroscopy (XPS) and electron paramagnetic resonance (EPR) spectroscopy indicates the presence of a O=V^{IV} species with V2p binding energy of 516 eV (Figure S45 in the Supporting Information) and EPR signals that are comparable to those reported for solid-supported vanadyl species (see Figure S46 in the Supporting Information for more details). Because the chelating catecholate ligand is dianionic, complexation of the O=V^{IV} moiety to it balances out the remaining charges so that additional coordinated ligand, if any, must be neutral. While it is possible that one or both of the neutral acetylacetonate (Hacac) ligands remain bound to the V center after metallation, we were unable to confirm their presence (or absence) using FTIR spectroscopy (Figure S48 in the Supporting Information) given the overlapping peaks in the 1500–1600 cm⁻¹ region of the spectra of the MOFs with those expected from the C=C bond of the conjugated α -carbonyl enol (~1526 cm⁻¹) and C=O (~1562 cm⁻¹) of the acac (quoted values are for VO(acac)₂). Indeed, the spectra of **CatBrO MOF** and the metallated **V-CatBrO MOF** are quite similar. However, the FTIR spectrum of a physical mixture of **CatBrO MOF** and VO(acac)₂ (0.35 mol %, to simulate the theoretical loading of one acac per vanadyl ion in MOF) exhibits a noticeable growth in the 1526–1560 cm⁻¹ region, relative to the adjacent 1620 cm⁻¹ peak, that is not seen in the spectrum **V-CatBrO MOF**, suggesting that either Hacac is not present in **V-CatBrO MOF** or that FTIR is insensitive to the small amount of Hacac in the sample. Nonetheless, even if a small amount of Hacac is still bound to the V center, we expect it to be labile enough for displacement by substrates or solvents during catalysis, leading to accessible open metal sites for catalysis.

Although a crystal structure of **V-CatBrO MOF** could not be obtained, its PXRD pattern indicates that the crystallinity of the starting **BOC-CatBrO MOF** was maintained throughout the two postsynthesis modification steps (Figure S43 in the Supporting Information). While similar sequences of modification have been carried out on derivatives of UMCM-1,³⁰ the catalytic utility of the resulting metallated MOFs was not

Scheme 2. A Schematic Illustration of the Synthesis of V-CatBrO MOF via Postsynthesis Deprotection Followed by Metallation^a

^aThe [V=O] notation represents a generic vanadyl ion and indicates the possibility that other coordinated ligands (solvent or neutral acetylacetonate) may exist around the V center.

demonstrated. However, Rosseinsky and co-workers have demonstrated that V-modified MOF, obtained by postsynthesis incorporation of VO(acac)₂ into salicylaldehyde-functionalized IR-MOF-3, is catalytically active for cyclohexene oxidation.⁵³ Thus, given the large pores of V-CatBrO MOF and the unsaturated (labile) coordination environment around its oxidation-capable V centers, we hypothesized that it would also be catalytically active in oxidation catalysis, particularly towards relatively large substrates. We chose to explore the benzylic oxidation of tetralin given that large porous MOFs such as MIL-101 have been shown to catalyze this reaction with high selectivity.^{54,55}

Catalysis. As expected, V-CatBrO MOF is catalytically active for the benzylic oxidation of tetralin in the presence of *tert*-butyl hydroperoxide (TBHP) oxidant (Figure 4). At 50 °C in chlorobenzene, tetralin was oxidized to mainly tetralol and tetralone (~1:3 molar ratio) at 45% total conversion by 24 h (Figure 4). This activity is comparable to that of the homogeneous VO(acac)₂, whose products comprise more of the overoxidized product tetralone (1:11 tetralol:tetralone ratio) at comparable overall total conversion (Figure 4). The PXRD pattern of V-CatBrO MOF after catalysis indicated that crystallinity is partially maintained, with great reduction in the intensity of the lowest angle peak and the appearance of additional peaks/noise (Figure S50 in the Supporting Information). Nonetheless, the porosity of the crystals as determined at TGA was preserved (Figure S51 in the Supporting Information), and the crystal size was unaffected by catalysis (Figure S52 in the Supporting Information).

Noncoordinating solvent such as chlorobenzene is the best medium for catalysis with V-CatBrO MOF because acetonitrile caused significant leaching of vanadium ions in our hands. Catalyst-filtration test (Figure 4) showed that the catalysis by V-CatBrO MOF in chlorobenzene is mostly heterogeneous with minimal contribution from any leached metal ions.⁵⁶ A control experiment using “metallated” BOC-CatBrO MOF (with a low 0.07 V/Zn ratio, see above) showed no catalytic activity at 4 h and only minimal activity after 24 h (only 4% tetralone and 2% tetralol yields, see Figure S49 in the Supporting Information), further supporting our hypothesis that the catalytic activity observed in V-CatBrO MOF is primarily due to the (catecholate)V=O moiety.

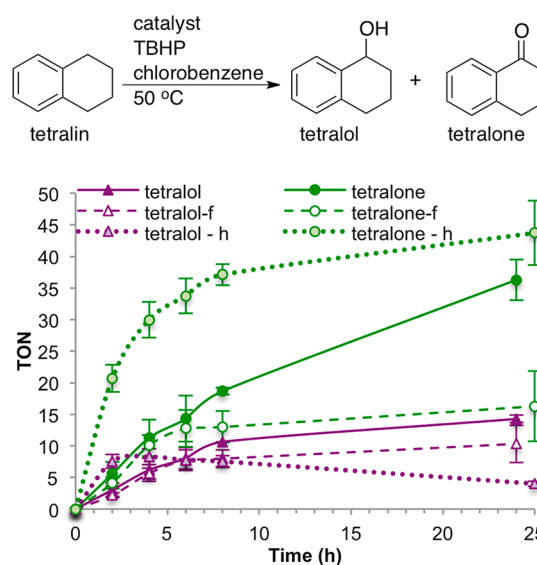


Figure 4. The reaction profile for the oxidation of tetralin into tetralol and tetralone using VO(acac)₂ or V-CatBrO MOF catalyst in the presence of TBHP. Reactions were carried out in chlorobenzene at 50 °C and at a 100:100:1 (or 0.75) molar ratio of tetralin:TBHP:catalyst. Exposing tetralin to TBHP alone under the same conditions does not result in oxidation. Catalysis profiles are designated as follow: solid lines, V-CatBrO MOF; dashed lines, the filtered-off (abbreviated as f) supernatant at 4 h in the reaction initially catalyzed by V-CatBrO MOF; dotted lines, homogeneous VO(acac)₂ (abbreviated as h). Products designation: tetralone, green circles; tetralol, purple triangles.

CONCLUSIONS

By using a combination of protecting groups, postsynthesis deprotection, and postsynthesis metallation, we were able to extend the pillared paddlewheel MOF platform system to display a novel and catalytically active vanadyl-(monocatecholate) motif that is inaccessible homogeneously. In our hands, the thermolabile BOC group offered traceless deprotection of BOC-CatBrO MOF to give crystalline CatBrO MOF with large pores that can be loaded with a high density of vanadyl ions. The resulting metallated MOF can catalyze the benzylic oxidation of a large substrate such as tetralin in the

presence of a bulky oxidant with minimal metal leaching in a noncoordinating solvent. These results point toward the potential of MOF as a support platform for homogeneously inaccessible coordination complexes that are competent for catalysis.

■ ASSOCIATED CONTENT

📄 Supporting Information

Materials and methods, ligand synthesis, NMR spectra of ligands, photographic images of MOFs, selected single-crystal X-ray diffraction data, TGA, CO₂ isotherms, NMR spectra of digested MOFs, ICP-OES data, PXRD patterns, and FTIR, XPS, and EPR spectra of PG-CatBrO MOF, CatBrO MOF, and V-CatBrO MOF. This material is available free of charge via the Internet at <http://pubs.acs.org>.

■ AUTHOR INFORMATION

Corresponding Author

*Tel.: 847-467-4934 (O.K.F.); 847-491-3504 (J.T.H.); 847-467-3347 (S.T.N.). Fax: 847-491-7713. E-mail: o-farha@northwestern.edu (O.K.F.); j-hupp@northwestern.edu (J.T.H.); stn@northwestern.edu (S.T.N.).

Author Contributions

M.H.W., O.K.F., J.T.H., and S.T.N. conceived the initial experiment. H.G.T.N. and M.H.W. carried out all of the experiments and measurements. A.A.S. solved the single crystal structures. Z.A. performed XPS measurements. M.R.W. supervised the EPR experiments and analysis performed by D.M.G. and R.C. O.K.F., J.T.H., and S.T.N. supervised the project. H.G.T.N. and M.H.W. wrote the initial drafts of the paper. H.G.T.N. and S.T.N. finalized the manuscript with contributions from all authors. All authors have given approval to the final version of this manuscript.

Funding

This work was supported by the Chemical Sciences, Geosciences, and Biosciences Division, Office of Basic Energy Sciences, U.S. Department of Energy (grant DEFG02-03ER15457 to the Institute of Catalysis for Energy Processes at Northwestern University (assistantship for H.G.T.N.) and grant no. DE-FG02-99ER14999 to M.R.W.). D.M.G. was supported by the Department of Defense through the National Defense Science & Engineering Graduate Fellowship (NDSEG) Program. R.C. was supported as part of the ANSER Center, an Energy Frontier Research Center funded by the U.S. Department of Energy (DOE), Office of Science, Office of Basic Energy Sciences, under award number DE-SC0001059.

Notes

The authors declare no competing financial interest.

■ ACKNOWLEDGMENTS

We thank the reviewers of the initial version of this manuscript for suggestions that greatly strengthened the final work.

■ REFERENCES

- (1) Yaghi, O. M.; O'Keeffe, M.; Ockwig, N. W.; Chae, H. K.; Kim, J. *Nature* **2003**, *423*, 705–714.
- (2) Férey, G. *Chem. Soc. Rev.* **2008**, *37*, 191–214.
- (3) Horike, S.; Shimomura, S.; Kitagawa, S. *Nat. Chem.* **2009**, *1*, 695–704.
- (4) Kitagawa, S.; Kitaura, R.; Noro, S.-i. *Angew. Chem., Int. Ed.* **2004**, *43*, 2334–2375.

- (5) Lee, J.; Farha, O. K.; Roberts, J.; Scheidt, K. A.; Nguyen, S. T.; Hupp, J. T. *Chem. Soc. Rev.* **2009**, *38*, 1450–1459.
- (6) Ma, L.; Abney, C.; Lin, W. *Chem. Soc. Rev.* **2009**, *38*, 1248–1256.
- (7) Lalonde, M.; Bury, W.; Karagiari, O.; Brown, Z.; Hupp, J. T.; Farha, O. K. *J. Mater. Chem. A* **2013**, *1*, 5453–5468.
- (8) Corma, A.; Garcia, H.; Llabres i Xamena, F. X. *Chem. Rev.* **2010**, *110*, 4606–4655.
- (9) Farrusseng, D.; Aguado, S.; Pinel, C. *Angew. Chem., Int. Ed.* **2009**, *48*, 7502–7513.
- (10) Dhakshinamoorthy, A.; Alvaro, M.; Garcia, H. *Chem. Commun.* **2012**, *48*, 11275–11288.
- (11) Yoon, M.; Srirambalaji, R.; Kim, K. *Chem. Rev.* **2011**, *112*, 1196–1231.
- (12) Schlichte, K.; Kratzke, T.; Kaskel, S. *Microporous Mesoporous Mater.* **2004**, *73*, 81–88.
- (13) Henschel, A.; Gedrich, K.; Kraehnert, R.; Kaskel, S. *Chem. Commun.* **2008**, *44*, 4192–4194.
- (14) Horike, S.; Dincă, M.; Tamaki, K.; Long, J. R. *J. Am. Chem. Soc.* **2008**, *130*, 5854–5855.
- (15) Cho, S.-H.; Ma, B.; Nguyen, S. T.; Hupp, J. T.; Albrecht-Schmitt, T. E. *Chem. Commun.* **2006**, *42*, 2563–2565.
- (16) Hu, A.; Ngo, H. L.; Lin, W. *J. Am. Chem. Soc.* **2003**, *125*, 11490–11491.
- (17) Shultz, A. M.; Farha, O. K.; Adhikari, D.; Sarjeant, A. A.; Hupp, J. T.; Nguyen, S. T. *Inorg. Chem.* **2011**, *50*, 3174–3176.
- (18) Shultz, A. M.; Farha, O. K.; Hupp, J. T.; Nguyen, S. T. *J. Am. Chem. Soc.* **2009**, *131*, 4204–4205.
- (19) Shultz, A. M.; Sarjeant, A. A.; Farha, O. K.; Hupp, J. T.; Nguyen, S. T. *J. Am. Chem. Soc.* **2011**, *133*, 13252–13255.
- (20) Song, F.; Wang, C.; Lin, W. *Chem. Commun.* **2011**, *47*, 8256–8258.
- (21) Suslick, K. S.; Bhyrappa, P.; Chou, J. H.; Kosal, M. E.; Nakagaki, S.; Smithenry, D. W.; Wilson, S. R. *Acc. Chem. Res.* **2005**, *38*, 283–291.
- (22) Takaishi, S.; DeMarco, E. J.; Pellin, M. J.; Farha, O. K.; Hupp, J. T. *Chem. Sci.* **2013**, *4*, 1509–1513.
- (23) Wu, C.-D.; Hu, A.; Zhang, L.; Lin, W. *J. Am. Chem. Soc.* **2005**, *127*, 8940–8941.
- (24) Wu, C.-D.; Lin, W. *Angew. Chem., Int. Ed.* **2007**, *119*, 1093–1096.
- (25) Chen, Y.; Lykourinou, V.; Hoang, T.; Ming, L.-J.; Ma, S. *Inorg. Chem.* **2012**, *51*, 9156–9158.
- (26) Zhang, Z.; Zhang, L.; Wojtas, L.; Nugent, P.; Eddaoudi, M.; Zaworotko, M. J. *J. Am. Chem. Soc.* **2011**, *134*, 924–927.
- (27) Alkordi, M. H.; Liu, Y.; Larsen, R. W.; Eubank, J. F.; Eddaoudi, M. J. *J. Am. Chem. Soc.* **2008**, *130*, 12639–12641.
- (28) Maksimchuk, N. V.; Timofeeva, M. N.; Melgunov, M. S.; Shmakov, A. N.; Chesalov, Y. A.; Dybtsev, D. N.; Fedin, V. P.; Kholdeeva, O. A. *J. Catal.* **2008**, *257*, 315–323.
- (29) Nguyen, H. G. T.; Weston, M. H.; Farha, O. K.; Hupp, J. T.; Nguyen, S. T. *CrystEngComm* **2012**, *14*, 4115–4118.
- (30) Tanabe, K. K.; Allen, C. A.; Cohen, S. M. *Angew. Chem., Int. Ed.* **2010**, *49*, 9730–9733.
- (31) Farha, O. K.; Shultz, A. M.; Sarjeant, A. A.; Nguyen, S. T.; Hupp, J. T. *J. Am. Chem. Soc.* **2011**, *133*, 5652–5655.
- (32) Chen, Y.; Hoang, T.; Ma, S. *Inorg. Chem.* **2012**, *51*, 12600–12602.
- (33) Meng, L.; Cheng, Q.; Kim, C.; Gao, W.-Y.; Wojtas, L.; Chen, Y.-S.; Zaworotko, M. J.; Zhang, X. P.; Ma, S. *Angew. Chem., Int. Ed.* **2012**, *51*, 10082–10085.
- (34) Pierpont, C. G.; Lange, C. W. *Prog. Inorg. Chem.* **2007**, *41*, 331–442.
- (35) Parallel work using porous organic polymer (POPs) decorated with catechol groups as supports for unsaturated metal coordination environment with applications in catalysis, gas storage, and removal of toxic chemicals can be found in the following references. (a) Weston, M. H.; Farha, O. K.; Hauser, B. G.; Hupp, J. T.; Nguyen, S. T. *Chem. Mater.* **2012**, *24*, 1292–1296. (b) Weston, M. H.; Peterson, G. W.; Browe, M. A.; Jones, P.; Farha, O. K.; Hupp, J. T.; Nguyen, S. T. *Chem. Commun.* **2013**, *49*, 2995–2997. (c) Tanabe, K. K.; Siladke, N. A.;

Broderick, E. M.; Kobayashi, T.; Goldston, J. F.; Weston, M. H.; Farha, O. K.; Hupp, J. T.; Pruski, M.; Mader, E. A.; Johnson, M. J. A.; Nguyen, S. T. *Chem. Sci.* **2013**, *4*, 2483–2489. (d) Kraft, S. J.; Sánchez, R. H.; Hock, A. S. *ACS Catal.* **2013**, *3*, 826–830.

(36) We note that Cohen and coworkers have incorporated protected-catechol struts into a derivative of UMCM-1 de novo, removed the protecting groups, and then metallated the free catechol groups with Fe(II). However, the metallated MOF was not demonstrated for catalytic capability. See: Tanabe, K. K.; Allen, C. A.; Cohen, S. M. *Angew. Chem., Int. Ed.* **2010**, *49*, 9730–9733.

(37) Farha, O. K.; Malliakas, C. D.; Kanatzidis, M. G.; Hupp, J. T. *J. Am. Chem. Soc.* **2009**, *132*, 950–952.

(38) We have previously incorporated a vanadyl(catecholate) moiety into MIL-101 (Cr) through postsynthesis modification and shown that it is catalytically active in sulfoxidation. However, we were only able to achieve surface modification. In addition, in exploring other oxidative reactions, such as allylic or benzylic oxidation, background catalysis from the unsaturated Cr metal centers interfered with our ability to distinguish catalysis resulting from the vanadyl(catecholate) moiety versus that from the coordinatively unsaturated Cr nodes. See: (a) Nguyen, H. G. T.; Weston, M. H.; Farha, O. K.; Hupp, J. T.; Nguyen, S. T. *CrystEngComm* **2012**, *14*, 4115–4118. (b) Kim, J.; Bhattacharjee, S.; Jeong, K.-E.; Jeong, S.-Y.; Ahn, W.-S. *Chem. Commun.* **2009**, *45*, 3904–3906. (c) Maksimchuk, N. V.; Kovalenko, K. A.; Fedin, V. P.; Kholdeeva, O. A. *Adv. Synth. Catal.* **2010**, *352*, 2943–2948. (d) Maksimchuk, N. V.; Kovalenko, K. A.; Fedin, V. P.; Kholdeeva, O. A. *Chem. Commun.* **2012**, *48*, 6812–6814.

(39) Nguyen, H. G. T., unpublished observations.

(40) Wuts, P. G. M.; Greene, T. W. *Greene's Protective Groups in Organic Synthesis*, 4th ed.; John Wiley & Sons, Inc.: Hoboken, NJ, 2007.

(41) Canivet, J.; Farrusseng, D. *ChemCatChem* **2011**, *3*, 823–826.

(42) Cohen, S. M. *Chem. Rev.* **2011**, *112*, 970–1000.

(43) Yamada, T.; Kitagawa, H. *J. Am. Chem. Soc.* **2009**, *131*, 6312–6313.

(44) Rankine, D.; Avellaneda, A.; Hill, M. R.; Doonan, C. J.; Sumbly, C. J. *Chem. Commun.* **2012**, *48*, 10328–10330.

(45) Canivet, J.; Aguado, S.; Bergeret, G.; Farrusseng, D. *Chem. Commun.* **2011**, *47*, 11650–11652.

(46) Gadzikwa, T.; Lu, G.; Stern, C. L.; Wilson, S. R.; Hupp, J. T.; Nguyen, S. T. *Chem. Commun.* **2008**, *44*, 5493–5495.

(47) Gadzikwa, T.; Farha, O. K.; Malliakas, C. D.; Kanatzidis, M. G.; Hupp, J. T.; Nguyen, S. T. *J. Am. Chem. Soc.* **2009**, *131*, 13613–13615.

(48) Deshpande, R. K.; Waterhouse, G. I. N.; Jameson, G. B.; Telfer, S. G. *Chem. Commun.* **2012**, *48*, 1574–1576.

(49) Allen, C. A.; Cohen, S. M. *J. Mater. Chem.* **2012**, *22*, 10188–10194.

(50) Sato, H.; Matsuda, R.; Sugimoto, K.; Takata, M.; Kitagawa, S. *Nat. Mater.* **2010**, *9*, 661–666.

(51) Deshpande, R. K.; Minnaar, J. L.; Telfer, S. G. *Angew. Chem., Int. Ed.* **2010**, *49*, 4598–4602.

(52) Lun, D. J.; Waterhouse, G. I. N.; Telfer, S. G. *J. Am. Chem. Soc.* **2011**, *133*, 5806–5809.

(53) Ingleson, M. J.; Perez Barrio, J.; Guilbaud, J.-B.; Khimyak, Y. Z.; Rosseinsky, M. J. *Chem. Commun.* **2008**, *44*, 2680–2682.

(54) Kockrick, E.; Lescouet, T.; Kudrik, E. V.; Sorokin, A. B.; Farrusseng, D. *Chem. Commun.* **2011**, *47*, 1562–1564.

(55) Kim, J.; Bhattacharjee, S.; Jeong, K.-E.; Jeong, S.-Y.; Ahn, W.-S. *Chem. Commun.* **2009**, *45*, 3904–3906.

(56) ICP analysis of the filtrate after 24 h of catalysis indicated that only 13% of V has leached.